Orbital mixing and ferromagnetism in $LaMn_{1-x}Ga_xO_3$

J.-S. Zhou and J. B. Goodenough
Texas Materials Institute, University of Texas at Austin, Austin, Texas 78712, USA
(Received 3 March 2008; revised manuscript received 23 April 2008; published 20 May 2008)

The competition between the quadratic term in a Jahn-Teller vibronic interaction and the structural bias in an orthorhombic perovskite induces orbital mixing. We show that orbital mixing rather than Jahn-Teller fluctuations is responsible for the ferromagnetism found in the perovskite system $LaMn_{1-x}Ga_xO_3$. We have also verified the model by resolving the local structural distortion obtained from a recent neutron-diffraction study.

DOI: 10.1103/PhysRevB.77.172409 PACS number(s): 75.30.Et, 71.70.Ej

Single-valent transition-metal perovskite oxides ABO_3 are normally antiferromagnetic; three-dimensional (3D) ferromagnetic coupling is rarely seen except in the double perovskites $A_2BB'O_6$ in which the B-site cations are ordered. The type-A antiferromagnetic order in the orthorhombic perovskite $LaMnO_3$ consists of ferromagnetic (001) planes coupled antiferromagnetically along the c axis. However, a transition to 3D ferromagnetic order is found[1,2] in $LaMn_{1-x}Ga_xO_3$ for $0.4<x<0.6$ even though the Ga^{3+} ion does not change the Mn^{3+}-ion valance. In order to understand the spin-spin interactions responsible for a particular magnetic order, a structural study is always essential, especially where local site distortions remove an orbital degeneracy, which is the case with high-spin, octahedral-site Mn^{3+}: t^3e^1 configurations. In $LaMnO_3$, the local site distortions intrinsic to the orthorhombic structure[3] bias ordering of the occupied e^1 orbital of Mn^{3+} into alternative bond axes of the (001) planes to give the observed type-A antiferromagnetic order as originally postulated.[4] A critical question is whether this Jahn-Teller (JT) orbital ordering at the Mn^{3+} ions is destroyed in the ferromagnetic phase of $LaMn_{1-x}Ga_xO_3$, which would imply a 3D ferromagnetic coupling by cooperative JT orbital fluctuations,[1] or whether local site distortions bias the orbital ordering so as to make orbital mixing responsible for the 3D ferromagnetism.

It is not possible to reveal the status of orbital ordering by simply monitoring the change of lattice parameters. In the orthorhombic perovskites RMO_3 (R=rare earth, M=transition metals: Y, Sc, Al, In, or Ga), the orthorhombic distortion can be measured by a strain parameter $S\equiv 2(b-a)/(b+a)$ that decreases continuously as the rare-earth ionic radius (IR) increases. The onset of the octahedral-site O_2-Mn-O_2 bond angle to $\alpha<90°$ at IR$\geq$1.11 Å suppresses the S factor dramatically and even makes $S<0$ in some orthorhombic perovskites,[5] e.g., in $LaGaO_3$. The continuous solid solution between $LaMnO_3$ with $S>0$ and $LaGaO_3$ with $S<0$ has $S\approx 0$ for some compositions of $LaMn_{1-x}Ga_xO_3$. The low-resolution x-ray diffraction data in 1961 led to the postulate[1] that the orbital degree of freedom is released in this JT active system where $S\approx 0$ holds. An orbital degree of freedom was believed to be responsible for the 3D ferromagnetic interaction. However, a recent experimental result[6] shows that magnetic ordering between Mn^{3+} ions in $LaMn_{0.5}Ga_{0.5}O_3$ collapses under a pressure $P\geq 8$ GPa where a phase transition to rhombohedral symmetry, which is incompatible with a cooperative JT distortion, takes place. This key observation rules out the possibility that opening an orbital degree of freedom results in ferromagnetic coupling. How a 3D ferromagnetic coupling is produced in a phase with cooperative JT distortions remains an open question. By taking into account the octahedral-site distortions resolved from a recent neutron diffraction study,[7] we show in this report that the ferromagnetic interaction in $LaMn_{1-x}Ga_xO_3$ is caused by orbital mixing.

Ferromagnetism occurs in a relatively narrow range of Ga doping, $0.4<x\leq 0.6$, in the phase diagram of $LaMn_{1-x}Ga_xO_3$; see Fig. 12 of Ref. 7. Figure 1 shows a well-defined ferromagnetic transition from measurements of the temperature dependence of magnetization and the isothermal M-H loop at 5 K of a $LaMn_{0.5}Ga_{0.5}O_3$ crystal. A spin-only saturation moment achieved at 5 K under $H=5$ T indicates a 3D ferromagnetic coupling that orders spins collinearly. The $M^{-1}(T)$ of the paramagnetic phase fits a Curie-Weiss law well. A positive Weiss constant means that ferromagnetic coupling exists in the phase up to at least room temperature, which allows us to study the origin of the ferromagnetic interaction from the structural data obtained at room temperature. The Mn-O bond lengths versus the Ga content in $LaMn_{1-x}Ga_xO_3$ taken from recent neutron diffraction data[7] are reproduced in Fig. 2(a). The bond-length splitting between the three Mn-O bonds in orthorhombic $LaMnO_3$ decreases as the Ga doping x increases and becomes negligible for $x>0.6$. The M-O bond-length splitting in the perovskite structure with $Pbnm$ space group can be caused by both the intrinsic structural distortion and orbital ordering. In order to distinguish contributions from these two sources, a polar plot of $\rho_0=(Q_2^2+Q_3^2)^{1/2}$ and $\phi=\tan^{-1}(Q_3/Q_2)$ (the angle opens anticlockwise from the Q_2 axis) has been made for $LaMn_{1-x}Ga_xO_3$, where the two

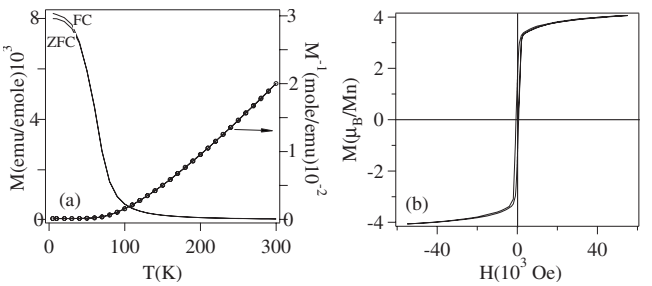

FIG. 1. (a) Temperature dependence of magnetization under 5000 Oe and (b) the isothermal magnetization at 5 K of a $LaMn_{0.5}Ga_{0.5}O_3$ crystal.

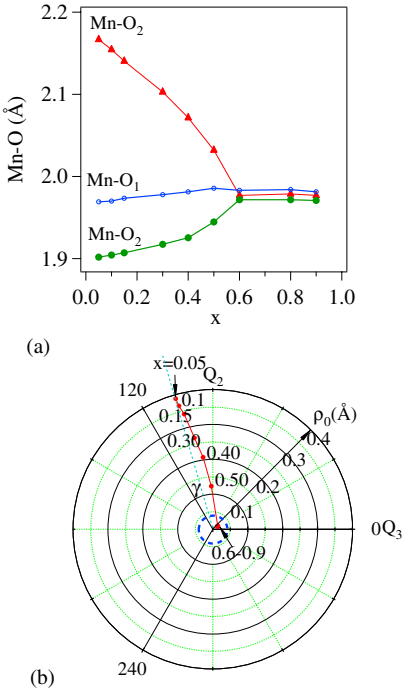

FIG. 2. (Color online) (a) The Ga doping dependence of the Mn-O bond lengths of $LaMn_{1-x}Ga_xO_3$ data are from Ref. 7; (b) the polar plot of $\rho_0=(Q_2^2+Q_3^2)^{1/2}$ and $\phi=\tan^{-1}(Q_3/Q_2)$ [$Q_2=l_x-l_y$ and $Q_3=(2l_z-l_x-l_y)/\sqrt{3}$], which are used to describe the octahedral-site distortion in the perovskites $LaMn_{1-x}Ga_xO_3$.

orthorhombic distortion modes are defined as $Q_2=\ell_x-\ell_y$ and $Q_3=(2\ell_z-\ell_x-\ell_y)/\sqrt{3}$ with the definition of the axes and unit cell given in Fig. 3. The ℓ_x, ℓ_y, and ℓ_z are Mn-O bond lengths along the respective bond axes. It should be noted that the definition of Q_2 and Q_3 with long, medium, and short bond lengths, which is widely used, may cause some problem since M-O bond lengths can become crossed as is seen in Fig. 2(a).

The description of the e electron in an MO_6 octahedron can be made by the wave function Ψ with a combination of orbitals $|x^2-y^2\rangle$ and $|z^2-r^2\rangle$ defined below in the Q_2, Q_3 space:

$$|x^2-y^2\rangle=\left(\tfrac{1}{2}r^2\right)(x^2-y^2),$$

$$|z^2-r^2\rangle=\tfrac{1}{3}(\sqrt{3}/2r^2)(3z^2-r^2),$$

$$\Psi(\theta)=\cos(\theta/2)|z^2-r^2\rangle+\sin(\theta/2)|x^2-y^2\rangle,$$

where the angle θ opens anticlockwise from the Q_3 axis. The fundamental reason why the angle dependence of Ψ is $\theta/2$ instead of θ was given by Sturge.[8] The wave function defined above includes orbital orderings along major bond axes in an orthorhombic MO_6 octahedron at special θ angles:

$$\Psi(0)=|z^2-r^2\rangle,\ \ \Psi(60)=|y^2-z^2\rangle,\ \ \Psi(120)=|y^2-r^2\rangle,$$

$$\Psi(180)=|x^2-y^2\rangle,\ \ \Psi(240)=|x^2-r^2\rangle,\ \ \Psi(300)=|z^2-x^2\rangle.$$

For an octahedral-site distortion that has a θ not falling at these special angles, whether the distortion reflects an orbital mixing or is simply caused by a combination of the orbital ordering with one of the special angles and the lattice orthorhombic distortion has been confused for a long time. Kanamori[9] noticed the deviation from $\theta=120°$ in $LaMnO_3$. Unfortunately, he attributed a $\phi\approx 11°$ to the second cause. This issue can be clarified if the magnitude of the intrinsic structural distortion is determined precisely. As seen in Fig. 2(b), which maps out ρ_0 and ϕ for site 1 in Fig. 3 of $LaMn_{1-x}Ga_xO_3$, all ϕ fall between the special angles, but close to 120° (it is close to 240° at site 3), and the magnitude of the octahedral-site distortion measured by ρ_0 falls continuously with increasing Ga doping x. The intrinsic structural distortion seen in $RFeO_3$ shows an interesting evolution of the site distortion as a function of the IR (Ref. 3); a maximum $\rho_0\approx 0.04$ Å occurs at IR ≈ 1.11 Å. The upper bound for the intrinsic structural distortion is shown as a dashed circle in the polar plot of Fig. 2(b). Only the ρ_0 for compositions $x\geq 0.6$ in $LaMn_{1-x}Ga_xO_3$ fall inside this circle. Therefore, it is clear that the octahedral-site distortion in compositions with $x<0.6$ reflects a contribution from a static JT orbital mixing. The evolution of the orbital mixing as a function of the IR or geometric tolerance factor t is influenced by the site structural bias effect as has been demonstrated by a close comparison between a non-JT $RFeO_3$ family and a JT active $RMnO_3$ family.[3,10] The difference in ρ_0 between these two families reflects the contribution from the JT orbital ordering in the $RMnO_3$ family; this difference is as high as an order of magnitude. It should also be emphasized here that there are no direct observations of orbital ordering and orbital mixing. The octahedral-site distortion we have discussed is compatible with orbital mixing. On the basis of our thorough description of the octahedral-site distortion and the justification for an orbital mixing, we are entitled to discuss the magnetic interaction as a consequence of the orbital mixing in $LaMn_{1-x}Ga_xO_3$.

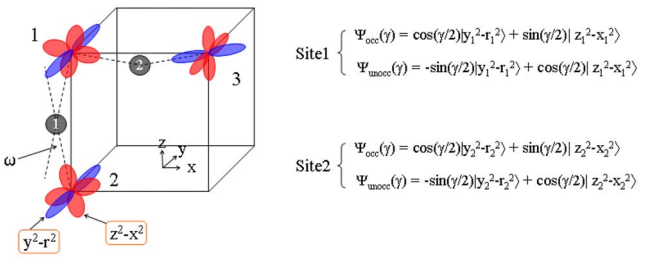

FIG. 3. (Color online) Schematic drawing of orbitals in the cubic unit cell of the perovskite structure. The octahedral-site rotation in the orthorhombic perovskite is shown by the angle ω.

Figure 3 illustrates a schematic drawing of Mn^{3+} ions and their orbitals in the $LaMnO_3$ lattice. Since the octahedral-site distortions of all members of $LaMn_{1-x}Ga_xO_3$ have the angle near 120° (240°), we choose to use the angle $\gamma=120°-\theta$ as defined in Fig. 2 and the corresponding wave function for convenience:

$$\Psi(\gamma)=\cos(\gamma/2)|y^2-r^2\rangle+\sin(\gamma/2)|z^2-x^2\rangle.$$

As long as γ stays below 30°, ferromagnetic coupling in an a-b plane due to the superexchange coupling between the

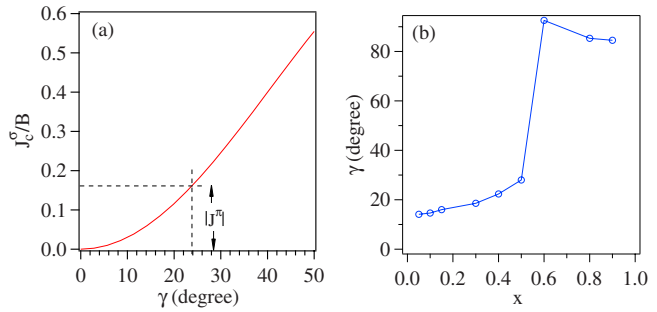

FIG. 4. (Color online) (a) The angle dependence of the σ-bond superexchange interaction along the c axis; (b) the angle in the Q_2-Q_3 plane for describing the octahedral-site distortion in $LaMn_{1-x}Ga_xO_3$. Data are from Ref. 7. Note that the bond-length splitting falls in the same level as the error bars for $x \geq 0.6$, which makes the angle determination uncertain in that doping range.

occupied orbital on site 3 and an empty orbital on site 1 should not be altered significantly. Therefore, we focus on whether the e-orbital magnetic coupling along the c axis due to an orbital mixing is ferromagnetic and whether it is large enough to offset the antiferromagnetic coupling through the π bonding.

For a given angle γ, wave functions of the occupied and unoccupied states for Mn^{3+} ions at sites 1 and 2 are listed in Fig. 3. The ferromagnetic coupling between the occupied state at site 1 and the unoccupied state at site 2 and *vice versa* is obtained as

$$J_F = B[2\ \sin(\gamma/2)\cos(\gamma/2)]^2,$$

$$B = \{\langle z_1^2 - x_1^2|H'|z_2^2 - x_2^2\rangle[\cos^4(\omega/2)]d^{3.5}\}^2/U,$$

where ω is defined in Fig. 3, d is the averaged Mn-O bond length, and U is the on-site correlation energy. The antiferromagnetic coupling between two occupied states at sites 1 and 2 is

$$J_{AF} = B\ \sin^4(\gamma/2).$$

The magnetic coupling between two unoccupied states at sites 1 and 2 is negligible since the virtual charge transfer involves the charge transfer gap Δ and U. Therefore, the superexchange interaction through the σ bond along the c axis is

$$J_c^\sigma = J_F - J_{AF} = \{[2\ \sin(\gamma/2)\cos(\gamma/2)]^2 - \sin^4(\gamma/2)\}B.$$

As seen in the plot of J_c^σ as a function of γ in Fig. 4, a ferromagnetic J_c^σ is obtained for $\gamma > 0$. However, a $J_c^\sigma > 0$ does not mean that a 3D ferromagnetic interaction is realized since the isotropic antiferromagnetic interaction J^π through t^3-O-t^3 must be overcome along the c axis. In order to have the values of J^π and the γ-independent J^σ, we have used the experimental result of $J_{ab} = J_{ab}^\sigma - J_{ab}^\pi = 1.67$ meV (Ref. 11) and an estimation of $J_c/J_{ab} \approx 1/4$ in $LaMnO_3$ by Millis.[12] We also notice that there should not be much difference between the two σ-bond orbital overlap integrals $\langle z_1^2 - x_1^2|H'|z_2^2 - x_2^2\rangle$ and $\langle z_1^2 - x_1^2|H'|x_3^2 - r_3^2\rangle$ and that J_c should be dominated by J_c^π in $LaMnO_3$. Therefore, we obtained $J_c^\pi \approx 0.4$ meV and $B \approx (d_2/d_1)^{3.5} J_{ab}^\sigma = 2.4$ meV, where $d_1 = 1.966$ Å and $d_2 = 2.04$ Å denote the Mn-O bond lengths along the c axis and the averaged Mn-O bond length within the ab plane, respectively. According to the plot of J_c^σ versus γ of Fig. 4(a), $J_c = J_c^\sigma - J_c^\pi > 0$ would occur at $\gamma > 24°$, which just falls between angles for the antiferromagnetic phase of $x = 0.4$ and the ferromagnetic phase of $x = 0.5$ shown in Fig. 4(b). Although this conclusion is made on the basis of some estimation and approximation, it highlights the possibility that a 3D ferromagnetic coupling can be achieved through orbital mixing.

The vibronic e states of an isolated JT-active molecule are degenerate in the Q_2-Q_3 plane; the e electrons move in the so-called "Mexican hat" potential. The quadratic term of the vibronic interaction converts the Mexican hat potential into one with three wells at $\theta = 0°$, 120°, and 240° (Ref. 13). The structural bias effect in the perovskite with *Pbnm* space group, which causes the site distortion as shown in $RFeO_3$ (Ref. 3), clearly removes the well at $\theta = 0°$ and moves the other two wells toward the Q_2 axis. It is very important to identify the competition between the quadratic term of the vibronic interaction and the structural bias effect in a solid. The transition to 3D ferromagnetism found in $LaMn_{1-x}Ga_xO_3$ is a direct consequence of this competition.

Neutron-diffraction results only give an averaged bond length and bond angle in this system with a mixture of JT active Mn^{3+} ions and non-JT Ga^{3+} ions. The overall reduction of the JT distortion by substitution of Ga^{3+} has been explained by an orbital ordering in which the Mn^{3+} ions nearby Ga^{3+} take $\Psi(0) = |z^2 - r^2\rangle$. This is the basis of an orbital-flipping model proposed by Farrell and Gehring.[14] Although the orbital ordering places some occupied orbitals along the c axis in order to give rise to a ferromagnetic coupling in this direction, the site distortion with $\theta = 0°$ is incompatible with the structural bias in the orthorhombic perovskites.

In conclusion, the ferromagnetism found in the $LaMn_{1-x}Ga_xO_3$ system has been rationalized with a model that takes into account the orbital mixing due to the structural bias effect in the perovskite structure with *Pbnm* space group. Predictions from the model match surprisingly well the experimental neutron-diffraction data for $LaMn_{1-x}Ga_xO_3$.

We thank the Robert A. Welch Foundation and the NSF for financial support.

[1] J. B. Goodenough, A. Wold, R. J. Arnott, and N. Menyuk, Phys. Rev. **124**, 373 (1961).
[2] J.-S. Zhou, H. Q. Yin, and J. B. Goodenough, Phys. Rev. B **63**, 184423 (2001).
[3] J.-S. Zhou and J. B. Goodenough, Phys. Rev. B **77**, 132104 (2008).
[4] J. B. Goodenough, Phys. Rev. **100**, 564 (1955).
[5] J.-S. Zhou and J. B. Goodenough, Phys. Rev. Lett. **94**, 065501 (2005).
[6] J.-S. Zhou *et al.* (unpublished).
[7] J. Blasco, J. Garcia, J. Campo, M. C. Sanchez, and G. Subias, Phys. Rev. B **66**, 174431 (2002).
[8] M. D. Sturge, in *Solid State Physics*, edited by F. Seitz, D. Turnbull, and H. Ehrenreich (Academic Press, New York, 1967), Vol. 20, p. 118.
[9] J. Kanamori, J. Appl. Phys. **31**, S14 (1960).
[10] A comparison between two perovskite families $R\mathrm{FeO}_3$ and $R\mathrm{MnO}_3$ has also been made by G. Maris, V. Volotchaev, and T. T. M. Palstra, New J. Phys. **6**, 153 (2004).
[11] R. Kajimoto, H. Mochizuki, H. Yoshizawa, H. Shintani, T. Kimura, and Y. Tokura, J. Phys. Soc. Jpn. **74**, 2430 (2005).
[12] A. J. Millis, Phys. Rev. B **55**, 6405 (1997).
[13] I. B. Bersuker, *Electronic Structure and Properties of Transition Metal Compounds: Introduction to the Theory* (Wiley, New York, 1996), p. 302.
[14] J. Farrell and G. A. Gehring, New J. Phys. **6**, 168 (2004).